Indonesian Journal of Electrical Engineering and Computer Science
Vol. 21, No. 3, March 2021, pp. 1611∼1621
ISSN: 2502-4752, DOI: 10.11591/ijeecs.v21i3.pp1611-1621

Sectoral dual-polarized MIMO antenna for 5G-NR band N77 base station

M. Muhsin[1], Afina Lina Nurlaili[2], Aulia Saharani[3], Indah Rahmawati Utami[4]
[1,3,4]Department of Telecommunication Engineering, Institut Teknologi Telkom Surabaya, Indonesia
[2]Department of Informatics, Universitas Pembangunan Nasional "Veteran" Jawa Timur, Indonesia

Article Info

Article history:

Received Oct 2, 2020
Revised Dec 2, 2020
Accepted Dec 23, 2020

Keywords:

5G
Antena
Correlation
Coupling
MIMO

ABSTRACT

Massive internet of things (IoT) in 5G has many advantages as a future technology. It brings some challenges such as a lot of devices need massive connection. In this case, multiple-input multiple-output (MIMO) systems offer high performance and capacity of communications. There is a challenge of correlation between antennas in MIMO. This paper proposes three-sectors MIMO base station antenna for 5G-New Radio (5G-NR) band N77 with dual polarized configuration to reduce the correlation. The proposed antenna has a maximum coupling of -16.90 dB and correlation below 0.01. The obtained bit error rate (BER) performance is very close to non-correlated antennas with bandwidth of 1.87 GHz. It means that the proposed antenna has been well designed.

Corresponding Author:

M. Muhsin
Department of Telecommunication Engineering
Institut Teknologi Telkom Surabaya
Jalan Ketintang 156, Surabaya, Indonesia
Email: muhsin@ittelkom-sby.ac.id

1. INTRODUCTION

Internet of things (IoT) is becoming a trend in the following year and future [1-4]. It has been started since the fourth generation of telecommunications (4G). In the next telecommunication generation, IoT is expected to grow more massively. Current IoT will be evolved into massive IoT, where there is more massive connectivity in the networks. Massive IoT in 5G is challenging because it should be able to accommodate a very high number of devices simultaneously. Capacity is main problem of massive IoT in 5G. It can be realized by provide high number of cell, each can handle a high volume of traffic [5, 6]. Massive traffic can be divided into some cells handling traffic in its coverage area. Each base station should use MIMO to provide enough capacity with high performance.

Multiple-input multiple-output (MIMO) is one of primary key for 5G [7-15] as enabler of massive IoT. Multiple antennas makes performance improvement where one antenna works together with other antennas. In order to gain the best performance, every antenna should be independent of each other. Independence is needed to provide optimum diversity. So, lowering dependency is one of the main focus in designing the MIMO antenna. It is because the dependency between antennas may decrease channel diversity which makes the system's performance worse. Dependency is indicated by antenna's correlation [16-19].

Depencency is measured by correlation between antennas. Some basic techniques have been proposed, for example, dual-cross polarized antenna on [20-23], ground decoupling on [24-27], sectorization on [28]. Dual-cross polarized antenna works by arranging the antenna so that the neighboring antenna has different polarization. Ground decoupling works by modifying the antenna's ground to reduce the antenna's interaction in the ground part. Sectorization works by arranging antennas having different focus of radiation pattern. Small cell base station for indoor dense networks is evaluated in [29-31]. Main characteristics of small cell 5G IoT base stations are MIMO and low coverage. This base station usually uses mm-Wave MIMO to provide high data rate and limited coverage. But, this technique has complexity disadvantages since mm-Wave devices are still uncommon and require additional configuration to work together with sub-6 GHz networks.

This paper proposes low-correlation MIMO antenna decoupling on 5G new radio (5G-NR) Band N77 using three sectors and dual-polarized configuration. It combines sectorization and dual-polarized techniques. These two techniques are combined to provide low correlation and dividing the cells. Sectorization is used for space diversity on each side and dual-polarized is used for polarization diversity. The antenna is designed and evaluated by coupling, correlation, and BER performance. The rest if this paper is organized as follows. Antenna design is presented in section 2 started from single antenna to three-sectors dual-polarized antenna. Simulation model is explained in section 3 Results are presented and discussed in section 4 and then, the conclusion is presented in section 5.

2. ANTENNA DESIGN

Antenna is designed in step by step basis from single antenna to 3-sectors dual-polarized MIMO antenna. Single antenna is used as a basic model. And then this design is extended to four-elements MIMO dual-polarized antenna in a plane. This 4-elements antenna is then extended to 3-sectors dual-polarized MIMO antenna.

2.1. Single Antenna

Circular patch microstrip antenna is selected as a basic model of single antenna. This type is chosen due to its simplicity. Basically, circular patch mictrostrip antennas have unidirectional radiation patterns, which can be suitable for each sector of sectoral antennas. Some dimensional parameters can be set to obtain the best performance of the antenna. This single antenna should be well designed because of its role as a basis for a full MIMO antenna. Rogers RT-5880 is used as antenna's material with thickness $h = 1.6$ mm. This material has relative permittivity $\epsilon_r = 2.2$ and superior performance compared to FR-4, which is suitable for ultra wide band (UWB) above 3 GHz [32-34]. Material characteristics of RT-5880 allows antenna's dimension to lower manufacturing error and high power capability. This material then designed to obtain the requirement of a single antenna in Table 1.

Table 1. Single antenna specification

Material	:	Rogers RT-5880
Relative Permittivity	:	2.2
Substrate's Thickness	:	1.6 mm
Conductor	:	Copper
Conductor's Thickness	:	35 μm
Frequency Range (5G N77)	:	3.3-4.2 GHz
Maximum Return Loss	:	-10 dB
Radiation Pattern Type	:	Unidirectional

Basically, the single antenna design is started from a simple circular disk microstrip antenna. The antenna has circular shaped disk with radius [35-37]:

$$r = \frac{F}{\sqrt{1 + \frac{2h}{\pi \epsilon_r F}\left[\ln\left(\frac{\pi F}{2h}\right) + 1.7726\right]}} \tag{1}$$

where

$$F = \frac{8.791 \times 10^9}{f\sqrt{\epsilon_r}}. \tag{2}$$

h is substrate's height/depth, f is resonant frequency, and ϵ_r is substrate's relative permittivity. The antenna is fed with microstrip line with width formulated in [38].

Formula in (1) didn't count fringing effect and other neglected factors. It means that the optimization is needed. Antenna's ground has been cut to provide wider bandwidth. By cutting the ground at certain section, impedance become wider and antenna's main lobe become smaller.

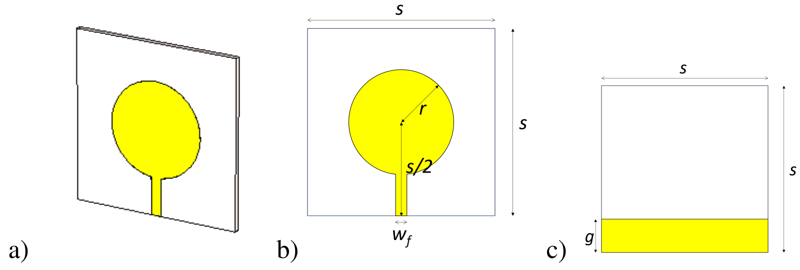

Figure 1. Single antenna: (a) 3D view, (b) Front view, (c) Back view

Optimized single antenna is shown in Figure 1. Disk radius r is 14 mm, feed's width w_f is 3 mm, ground plane's length g is 10 mm, and single antenna's plane s is 50 mm.

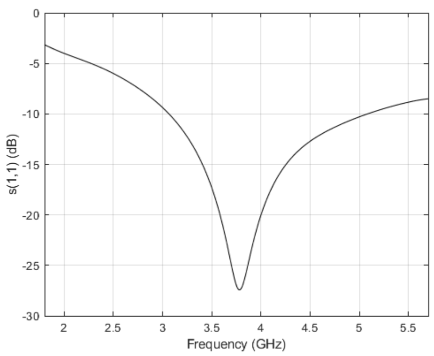

Figure 2. Return loss of single antenna

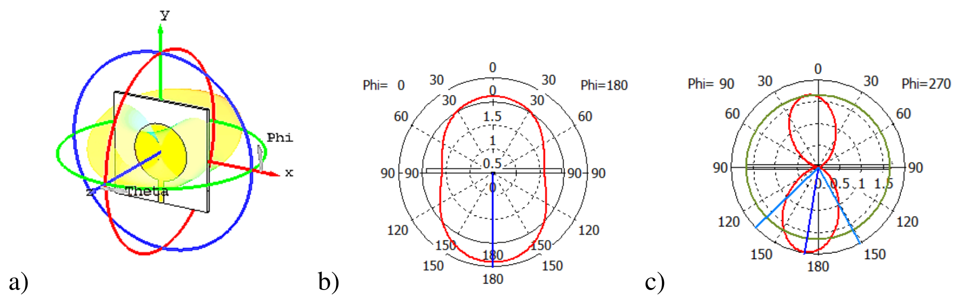

Figure 3. Radiation pattern of single antenna: (a) 3D, (b) Azimuth, (c) Elevation

Requirement on Table 1 must been met by the single antenna designed. Obtained port reflection coefficient is shown in Figure 2. The antenna works between 3.06 GHz and 5.08 GHz with return loss below -10 dB [36] and 2.08 GHz bandwidth. It means that frequency range or bandwidth requirement has been met. Obtained radiation pattern is shown in Figure 3. It has been shown that the antenna has unidirectional radiation pattern with 2.921 dBi gain at 3.7 GHz with -0.01686 dB radiation efficiency. It means that radiation pattern requirement has been met.

2.2. Dual Polarized Antenna

Antenna from section 2.1. is the basic for dual polarized antenna design. The single antenna is duplicated then arranged with dual polarized configuration as seen in Figure 4. Neighboring antennas have different orthogonal polarization. Crossing antennas have same polarization with different direction of feeding. This configuration is made to reduce coupling and correlation between antennas [20-23, 16-18].

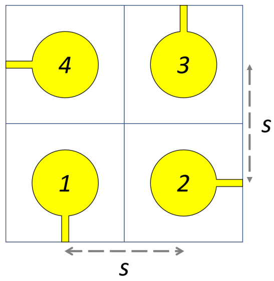

Figure 4. Dual polarized antenna

2.3. Three Sectors Antenna

Dual polarized antenna in section 2.2. then extended into three-sectors MIMO antenna. Each sector is composed from one dual-polarized antenna with sector radius $r_c = 50$ mm. Each sector serves users or subscribers in respective sectors. Three sectors are made based on conventional sectoral antennas for mobile communications (Figure 5).

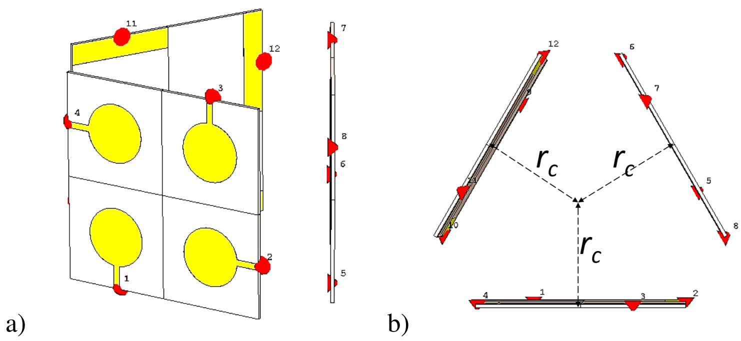

Figure 5. 3 Sectors antenna: (a) 3D view, (b) Upper view

3. SIMULATION MODEL

In this section, a simulation model of the system using designed antennas is explained. Simulation is used to demonstrate MIMO antenna's performance in the communication systems. The simulation involves correlation between antennas as one of input parameters. Result of the simulation is BER performance compared to ideal non-correlated MIMO antennas. Quasi-Orthogonal space-time block codes (QOSTBC) is used as MIMO coding with a coding rate of $R = 1$. And then QOSTBC is implemented in a correlated MIMO channel. To simplify the simulation, equivalent virtual channel matrix (EVCM) is used in the system's simulation.

3.1. Quasi-Orthogonal Space-Time Block Codes

QOSTBC offers full rate space-time block codes for high number of antennas [39-42]. Basic QOSTBC uses an extension of Alamouti Space-Time Block Codes (STBC). If Alamouti coded signal of x_1 and x_2 is:

$$A = C_{2\times 2}\left(x_1, x_2\right) = \begin{pmatrix} x_1 & x_2 \\ -x_2^* & x_1^* \end{pmatrix} \tag{3}$$

and Alamouti coded signal of x_3 and x_4 is

$$B = C_{2\times 2}\left(x_3, x_4\right) = \begin{pmatrix} x_3 & x_4 \\ -x_4^* & x_3^* \end{pmatrix}, \tag{4}$$

Extended Alamouti Quasi-Orthogonal Space-Time Block Codes (EA-QOSTBC) of x_1, x_2, x_3, and x_4 is

$$C_{4\times 4}(x_1, x_2, x_3, x_4) = \begin{pmatrix} A & B \\ -B^* & A^* \end{pmatrix}. \tag{5}$$

By substituting (3) and (4) to (5),

$$C_{4\times4}(x_1,x_2,x_3,x_4)=\begin{pmatrix} x_1 & x_2 & x_3 & x_4 \\ -x_2^* & x_1^* & -x_4^* & x_3^* \\ -x_3^* & -x_4^* & x_1^* & x_2^* \\ x_4 & -x_3 & -x_2 & x_1 \end{pmatrix}. \tag{6}$$

EA-QOSTBC in (6) has full rate characteristics with orthogonality of $3/4$.

3.2. Correlated MIMO channel

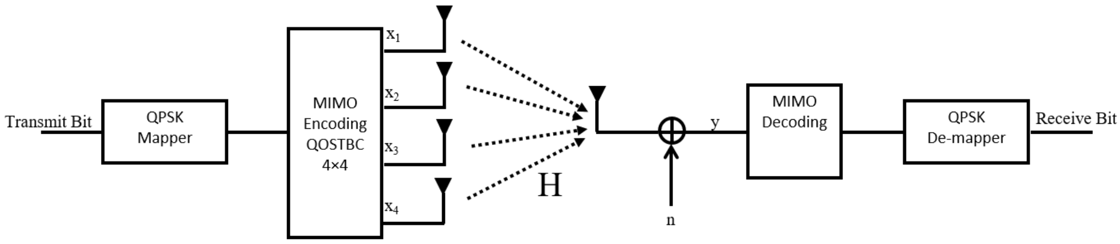

Figure 6. MIMO 4×1 systems using QOSTBC 4×4 with QPSK modulation

Simulation system in this paper is shown in Figure 6. In an ideal situation, the channel H is independent for each corresponding transmit and receive antennas. Independent or uncorrelated channels provide maximum diversity in the systems. Received signal of the MIMO channel is expressed as [43, 44]:

$$y = Hx + n \tag{7}$$

with H is $N_r \times N_t$ channel matrix, x is transmitted signal, and n is additive white Gaussian noise (AWGN). Number of transmit and receive antennas are N_t and N_r, respectively. In this research, MIMO channel matrix is:

$$H = \begin{pmatrix} h_1 & h_2 & h_3 & h_4 \end{pmatrix}. \tag{8}$$

Independent or orthogonal characteristics in (8) is defined by H and x. MIMO channel matrix H should be independent of each other which means each signal propagates through an independent channel. MIMO encoded transmit signal $\mathbf{x}$ should be generated by orthogonal MIMO coding. Correlated MIMO channel is modeled using Kronecker model as [45]:

$$H = R_r^{\frac{1}{2}} \times H_{\text{i.i.d}} \times R_t^{\frac{1}{2}} \tag{9}$$

with R_r is receiver's correlation matrix, $H_{\text{i.i.d}}$ is independent and identically distributed (i.i.d) channel matrix, and R is transmitter's correlation matrix. Both R_t and R_r are equivalently dependent on the antenna's parameter. In this research, $N_r = 1$ because there is only one receive antenna.

3.3. Equivalent Virtual Channel Matrix

EVCM is used to simplify the MIMO system model. It works by transforming coded transmitted signals to the channel [18]. Assuming quasi-static flat-fading channel, $N_t \times 1$ can be simplified with receive signal vector [46]:

$$y_{\text{eq}} = C_h x + v \tag{10}$$

with C_h is $N_c \times N_t$ STBC coded channel matrix of h, x is transmit signal, v is equivalent AWGN, and N_c is length of MIMO coding. Coded channel matrix is expressed as:

$$h = \begin{bmatrix} h_1 & h_2 & h_3 & \cdots & h_{N_c} \end{bmatrix}^{\text{T}} \tag{11}$$

and transmit signal is expressed as:

$$x = \begin{bmatrix} x_1 & x_2 & x_3 & \cdots & x_{N_t} \end{bmatrix}^{\text{T}}. \tag{12}$$

4. RESULTS AND DISCUSSION

4.1. Coupling

In an array antenna, input from an antenna will affect output of another antenna. This parameter is described by coupling. If the antenna is indexed by i and j, output of antenna i from input of antenna j is $s_{i,j}$ where $i \neq j$. For antenna in Figure 5 the coupling matrix is:

$$S = \begin{pmatrix} s_{1,1} & s_{1,2} & s_{1,3} & \cdots & s_{1,12} \\ s_{2,1} & s_{2,2} & s_{2,3} & \cdots & s_{2,12} \\ s_{3,1} & s_{3,2} & s_{3,3} & \cdots & s_{3,12} \\ \vdots & \vdots & \vdots & \ddots & \vdots \\ s_{12,1} & s_{12,2} & s_{12,3} & \cdots & s_{12,12} \end{pmatrix} \tag{13}$$

where $s_{i,j}$ with $i = j$ is return loss of antenna $i = j$. Ideal value of S is for all $s_{i,j}$. In this case, there are 66 pairs of s_{ij} because there are 66 S_{ij} where $i \neq j$.

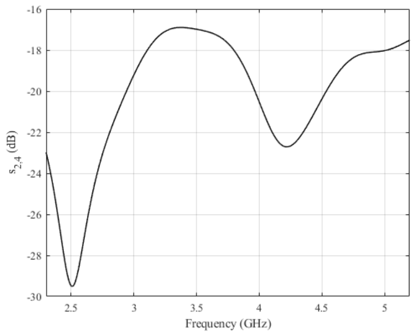

Figure 7. Coupling between antenna 2 and 4

Maximum coupling from frequency $3.3 - 4.2$ GHz is -16.90 dB between antenna 2 and 4 at 3.376 GHz. Maximum coupling at 3.7 GHz is -17 dB between antenna 2 and 4. $s_{1,4}$ is shown in Figure 7. Coupling between antenna 2 and 4 is relatively higher due to opposite feeding. Same values are pairs $(6, 8)$ and $(10, 12)$. These values are then evaluated by ECC in section 4.3.

4.2. Bandwidth

Return loss can be used to define bandwidth with the definition that the antenna works with maximum return loss of -10-dB. Based on (13), non diagonal elements of S represent coupling and diagonal elements of S represent return loss. Because of coupling, it also has an impact on antenna's return loss. Final 12 antennas in 3 sectors in section 2.3. have different bandwidth compared to single antennas in section 2.1. Return loss of 3 sectors antenna in section 2.3. has been shown in Figure 8. Limiting return loss from antenna 1 and 12 determined overall bandwidth. Antenna 1 has the highest lower threshold at 3.02 GHz and antenna 2 has the lowest upper threshold at 4.89 GHz. The antenna has 1.87 GHz bandwidth based on the return loss threshold -10 dB. Bandwidth of the antenna is decreased due to the antenna's coupling. It is usually happen on MIMO array antenna. The designed antenna should have a minimum bandwidth of 900 MHz with working frequency between $3.3 - 4.2$ GHz. Antenna reaches a bandwidth of 1.87 GHz with working frequency between $3.02 - 4.89$ GHz. Based on these values, the antenna can work on the required frequency and meet the requirement.

4.3. Correlation

Ideal MIMO antenna has no correlation between its elements. But, in reality, there are correlations. This correlation is usually measured using envelope correlation coefficient (ECC). ECC is defined by analyzing antennas' radiation pattern and polarization in spherical coordinates. ECC between antenna 1 and 2 is defined as [47]:

$$\rho_{e(1,2)} = \frac{\int\int \overline{F}_1 \cdot \overline{F}_2^* d\Omega^2}{\int\int \overline{F}_1^2 d\Omega \int\int \overline{F}_2^2 d\Omega} \tag{14}$$

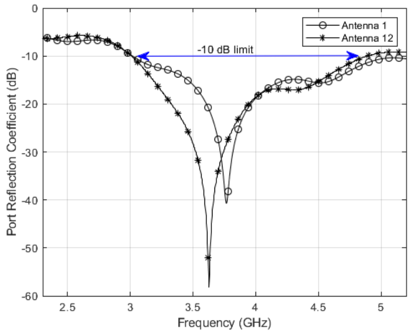

Figure 8. Port reflection coefficient of antenna 1 and 12

where F_1 and F_2 is complex radiation pattern of antenna 1 and antenna 2, respectively. Ω is azimuth and elevation orientation of the antenna.

ECC in (14) is very complex and hard to analyze. For high efficiency antennas, ECC between antenna 1 and 2 can be approached from isolation or coupling parameter as [48]:

$$\rho_{1,2} = \frac{\left|s_{1,1}^{*} s_{1,2} + s_{2,1}^{*} s_{2,2}\right|^2}{\left(1-\left(\left|s_{1,1}\right|^2+\left|s_{2,1}\right|^2\right)\right)\left(1-\left(\left|s_{jj}\right|^2+\left|s_{1,2}\right|^2\right)\right)}. \tag{15}$$

Non-correlated antenna pairs have ECC of 0 and fully correlated antenna pairs have ECC of 1. Value of ECC has a relation with diversity gain. Diversity gain is:

$$G_{\text{div}(1,2)} = 10\sqrt{1-\left|\rho_{\text{env}(1,2)}\right|} \tag{16}$$

Based on (16), smaller ECC means better diversity. There is a requirement of ECC $\rho \leq 0.5$ for a minimum effective diversity system. ECC comparison of single polarized and dual polarized antenna is shown in Figure 9. It has been seen that dual polarized antenna has been proven providing lower correlation compared to single polarized antenna. These characteristics are due to polarization diversity in dual polarized antennas which neighboring antennas have different orthogonal polarization.

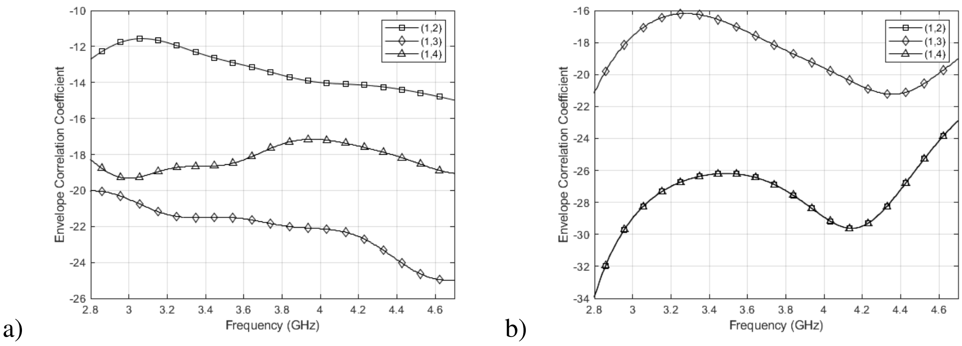

Figure 9. ECC of the: (a) Single polarized antenna, (b) Dual polarized antenna.

In the final designed antenna, there are 66 pairs of ECC. Antenna 1 has symmetry with odd numbered antennas and antenna 2 has symmetry with even numbered antennas. Considering symmetry of the designed antenna, ECC of antenna 1 with antenna $2, 3, ..., 12$ and antenna 2 with antenna $3, 4, ..., 12$ are enough to represent all 66 pairs. ECC pairs from antenna 1 and 2 are shown in Figure 10. Correlations in operation frequency $3.3 - 4.2$ GHz are below 10^{-2}. This correlation value is very low below the requirement of ECC Based on the ECC requirement of $\rho \leq 0.5$. It means that the antenna can provide performance close to non-correlated MIMO Antenna. These correlations are then evaluated in section 4.4. by using computer simulation of point-to-point communication systems.

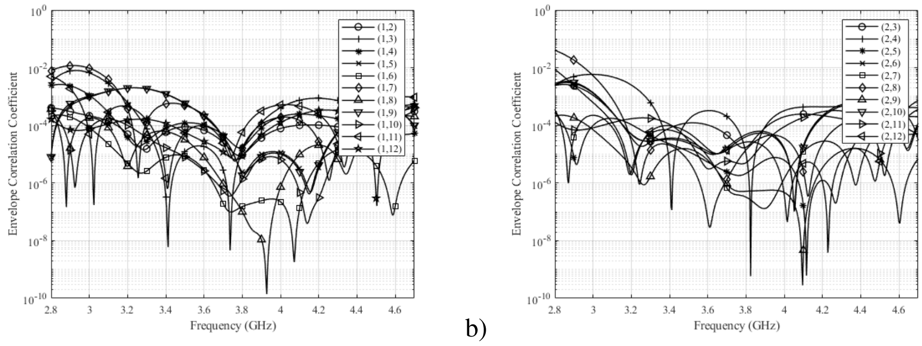

Figure 10. ECC of the final antenna: (a) Pairs of $(1, j)$, (b) Pairs of $(2, j)$

4.4. Performance of 4 x 1 System

The antenna tested in 4×1 MIMO system in Figure 6. Each sector with $120°$ angle is served by 4 antennas in a single sector. The simulation used quadrature phase shift keying (QPSK) and 4×4 QOSTBC as in section 3.1. Correlation as in section 4.3. is used based on correlated MIMO channels in section 3.2. and EVCM in section 3.3.

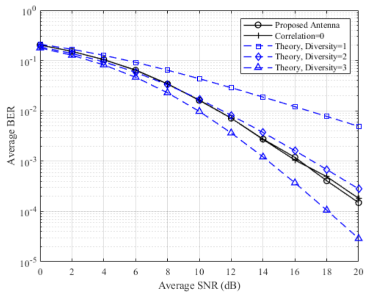

Figure 11. BER performances of the proposed antenna compared to ideal dully independent antenna and theoretical BER using MRC

Performance of the antenna is close to diversity order of 3. Theoritically, 4 transmit MIMO antenna with 1 receive antenna has performance on diversity order of 4. Reference BER for diversity order M is [49, 50]:

$$\bar{P}_b = \left(\frac{1-\Gamma}{2}\right)^M \sum_{m=0}^{M-1} \binom{M-1+m}{m} \left(\frac{1+\Gamma}{2}\right)^m \tag{17}$$

with

$$\Gamma = \sqrt{\frac{\overline{\mathrm{SNR}}}{2M + \overline{\mathrm{SNR}}}}. \tag{18}$$

where $\overline{\mathrm{SNR}}$ is average signal to noise ratio.

BER performance of the antenna in Figure 11 didn't reach a diversity order of 4 due to non-orthogonal STBC used. 4×4 QOSTBC has an orthogonality rate of $3/4$.

It is shown in Figure 11 that the BER of the antenna is very close to a fully independent antenna as reference. It confirmed that correlation in section 4.3. has very close performance to ideal antennas due to very low correlation. It also confirmed that the designed antenna has very good performance which is proven by its BER performance, although non-optimum diversity order reached due to non-fully-orthogonal STBC.

5. CONCLUSION

Three-sectors dual-polarized antenna for 5G-NR N77 has been proposed. The designed antenna has been evaluated by its coupling, bandwidth, correlation, and BER performance on 4×1 MIMO systems. The antenna has a bandwidth of 1.87 GHz with working frequency between 3.02 GHz and 4.89 GHz. Dual-cross polarization is used to minimize coupling in a single sector with maximum coupling of -16.90 dB at 3.376 GHz between antenna 2. Very low coupling leads to very low correlation between antennas. BER performance of the antenna is very close to fully independent antenna using 4×4 QOSTBC. Achieved diversity order using QOSTBC is close to 3 due to non-orthogonal MIMO coding.

REFERENCES

[1] S. Li, L. Da Xu, and S. Zhao, “5g internet of things: a survey,” *Journal of Industrial Information Integration*, vol. 10, pp. 1–9, 2018.

[2] D. Do and D. Nguyen, “The maximal sinr selection mode for 5g millimeter-wave mimo: Model systems and analysis,” *Indones. J. Electr. Eng. Comput. Sci*, vol. 7, no. 1, pp. 150–157, 2017.

[3] C. X. Mavromoustakis, G. Mastorakis, and J. M. Batalla, “Internet of Things (IoT) in 5G mobile technologies,” *Internet of Things (IoT) in 5G mobile technologies. Springer*, vol. 8, 2016.

[4] M. R. Palattella, M. Dohler, A. Grieco, G. Rizzo, J. Torsner, T. Engel, and L. Ladid, “Internet of things in the 5g era: Enablers, architecture, and business models,” *IEEE Journal on Selected Areas in Communications*, vol. 34, no. 3, pp. 510–527, 2016.

[5] F. Al-Turjman, E. Ever, and H. Zahmatkesh, “Small cells in the forthcoming 5g/iot: traffic modelling and deployment overview,” *IEEE Communications Surveys Tutorials,*, vol. 21, no. 1, pp. 28–65, 2018.

[6] A. Ijaz, L. Zhang, M. Grau, A. Mohamed, S. Vural, A. U. Quddus, M. A. Imran, C. H. Foh, and R. Tafazolli, “Enabling massive iot in 5g and beyond systems: Phy radio frame design considerations,” *IEEE Access*, vol. 4, pp. 3322–3339, 2016.

[7] P. Varzakas, “Average channel capacity for rayleigh fading spread spectrum mimo systems,” *International Journal of Communication Systems*, vol. 19, no. 10, pp. 1081–1087, 2006.

[8] Y. Rahayu, I. P. Sari, D. I. Ramadhan, and R. Ngah, “High gain 5g mimo antenna for mobile base station.”*International Journal of Electrical Computer Engineering* (2088-8708), vol. 9, no. 1, p. 468, 2019.

[9] E. G. Larsson, O. Edfors, F. Tufvesson, and T. L. Marzetta, “Massive mimo for next generation wireless systems,” *IEEE Communications Magazine*, vol. 52, no. 2, pp. 186–195, 2014.

[10] L. Lu, G. Y. Li, A. L. Swindlehurst, A. Ashikhmin, and R. Zhang, “An overview of massive mimo: Benefits and challenges,” *IEEE journal of selected topics in signal processing*, vol. 8, no. 5, pp. 742–758, 2014.

[11] T. L. Marzetta, Fundamentals of massive MIMO, *Cambridge University Press*, 2016.

[12] E. Bjornson, E. G. Larsson, and T. L. Marzetta, “Massive mimo: ten myths and one critical question,” *IEEE Communications Magazine,*, vol. 54, no. 2, pp. 114–123, 2016.

[13] T. L. Marzetta, “Massive mimo: an introduction,” *Bell Labs Technical Journal*, vol. 20, pp. 11–22, 2015.

[14] M. Agiwal, N. Saxena, and A. Roy, “Towards connected living: 5g enabled internet of things (IOT),” *IETE Technical Review,*, vol. 36, no. 2, pp. 190–202, 2019.

[15] L. Chettri and R. Bera, “A comprehensive survey on internet of things (IOT) towards 5g wireless systems,” *IEEE Internet of Things Journal*, vol. 7, no. 1, pp. 16-32, 2019.

[16] Muhsin, R. P. Astuti, and B. S. Nugroho, “Dual polarized antenna decoupling for 60 ghz planar massive mimo,” in *International Conference on Signals and Systems (ICSig Sys). IEEE*, pp. 158–162, 2017.

[17] Muhsin and K. Anwar, “Abba dual-cross-polarized antenna decoupling for 5g 16-element planar mimo at 28 ghz,” in *2018 2nd International Conference on Telematics and Future Generation Networks (TAFGEN). IEEE*, pp. 1–6 , 2018.

[18] M. Muhsin and R. P. Astuti, “Dual-cross-polarized antenna decoupling for 43 ghz planar massive mimo in full duplex single channel communications,” *International Journal of Advanced Computer Science and Applications*, vol. 10, no. 4, pp. 364–370, 2019.

[19] M. Muhsin, W. M. Hadiansyah, A. P. Pramita, and R. D. N. Cahyanti, “Planar dipole mimo array antenna for mobile robot communications at 5.6 ghz,” in *J2019 4th International Conference on Information Technology, Information Systems and Electrical Engineering (ICITISEE). IEEE*,pp. 244–248, 2019.

[20] A. Alfakhri, M. A. Ashraf, A. Alasaad, and S. Alshebeili, “Design and analysis of compact size dual

polarised ultra wideband mimo antennas with simple decoupling structure," in *Journal of Industrial Information Integration*, pp. 1–4, 2016.
[21] S. Saxena, B. K. Kanaujia, S. Dwari, S. Kumar, and R. Tiwari, "A compact dual-polarized mimo antenna with distinct diversity performance for uwb applications," In *2016 21st International Conference on Microwave, Radar and Wireless Communications (MIKON). IEEE*, vol. 16, pp. 3096–3099, 2017.
[22] N. O. Parchin, Y. I. A. Al-Yasir, A. H. Ali, I. Elfergani, J. M. Noras, J. Rodriguez, and R. A. Abd-Alhameed, " *IEEE Antennas and Wireless Propagation Letters*,, vol. 7, pp. 15 612–15 622, 2019.
[23] A. Moradikordalivand, T. A. Rahman, C. Y. Leow, and S. Ebrahimi, "Dual-polarized mimo antenna system for wifi and lte wireless access point applications," *IEEE Access*, vol. 30, no. 1, p. e2898, 2017.
[24] D. Wu, S. W. Cheung, Q. L. Li, and T. I. Yuk, "Decoupling using diamond-shaped patterned ground resonator for small mimo antennas," *IET Microwaves, Antennas Propagation*, vol. 11, no. 2, pp. 177–183, 2017.
[25] T. Shabbir, R. Saleem, A. Akram, and M. F. Shafique, "Uwb-mimo quadruple with fss-inspired decoupling structures and defected grounds," *Applied Computational Electromagnetics Society Journal*, vol. 30, no. 2, pp. 184–190, 2015.
[26] S. Zhang, X. Chen, and G. F. Pedersen, "Mutual coupling suppression with decoupling ground for massive mimo antenna arrays," *IEEE Transactions on Vehicular Technology* , vol. 68, no. 8, pp. 7273–7282, 2019.
[27] Z. Tang, J. Zhan, X. Wu, Z. Xi, and S. Wu, "Simple ultra-wider-bandwidth mimo antenna integrated by double decoupling branches and square-ring ground structure," *Microwave and Optical Technology Letters*, vol. 62, no. 3, pp. 1259–1266, 2020.
[28] S. S. Jehangir and M. S. Sharawi, "A wideband sectoral quasi-yagi mimo antenna system with multibeam elements," *IEEE Transactions on Antennas and Propagation*, vol. 67, no. 3, pp. 1898–1903, 2018.
[29] D. Muirhead, M. A. Imran, and K. Arshad, "Insights and approaches for low-complexity 5g small-cell base-station design for indoor dense networks," *EEE access*, vol. 3, pp. 1562–1572, 2015.
[30] M. H. Alsharif and R. Nordin, "Evolution towards fifth generation (5g) wireless networks: Current trends and challenges in the deployment of millimetre wave, massive mimo, and small cells," *Telecommunication Systems*, vol. 64, no. 4, pp. 617–637, 2017.
[31] W. Zhang, Y. Wei, S. Wu, W. Meng, and W. Xiang, "Joint beam and resource allocation in 5g mmwave small cell systems," In *IEEE Transactions on Vehicular Technology*, vol. 68, no. 10, pp. 10 272–10 277, 2019.
[32] R. K. Jaiswal, K. Kumari, and K. V. Srivastava, "Cavity backed co-radiator dual polarized mimo antenna," in *2019 IEEE Asia-Pacific Microwave Conference (APMC)*, pp. 792–794, 2019.
[33] N. Ojaroudiparchin, M. Shen, G. Fr et al., "Multi-layer 5g mobile phone antenna for multi-user mimo communications," in *015 23rd Telecommunications Forum Telfor (TELFOR). IEEE*, pp. 559– 562, 2015.
[34] M. I. Khattak, A. Sohail, U. Khan, Z. Barki, and G. Witjaksono, "Elliptical slot circular patch antenna array with dual band behaviour for future 5g mobile communication networks," *Progress In Electromagnetics Research*, vol. 89, pp. 133–147, 2019.
[35] C. Balanis, "Handbook of microstrip antennas," , 1982.
[36] C. A. Balanis, Antenna theory: analysis and design. John wiley sons, 2016.
[37] Modern antenna handbook. John Wiley Sons, 2008.
[38] D. M. Pozar, Microwave engineering. John wiley sons, 2009.
[39] H. Jafarkhani, "A quasi-orthogonal space-time block code," *IEEE Transactions on Communications*, vol. 49, no. 1, pp. 1–4, 2001.
[40] W. Su and X.-G. Xia, "Signal constellations for quasi-orthogonal space-time block codes with full diversity," *EEE Transactions on Information Theory,* , vol. 50, no. 10, pp. 2331–2347, 2004.
[41] Su, Weifeng, and X-G. Xia"Quasi-orthogonal space-time block codes with full diversity," *Global Telecommunications Conference, 2002. GLOBECOM'02. IEEE*, vol. 2. IEEE, pp. 1098–1102, 2002.
[42] A. Lotfi-Rezaabad, S. Talebi, and A. Chizari, "Two quasi orthogonal space-time block codes with better performance and low complexity decoder," in *2016 10th International Symposium on Communication Systems*, pp. 1–5 , 2016.
[43] G. Tsoulos, MIMO system technology for wireless communications. 2006.
[44] M. A. Jensen and J. W. Wallace, "A review of antennas and propagation for mimo wireless communications," *IEEE Transactions on antennas and propagation*, vol. 52, no. 11, pp. 2810–2824, 2004.
[45] E. A. Jorswieck and H. Boche, "Channel capacity and capacity-range of beamforming in mimo wireless

systems under correlated fading with covariance feedback," *IEEE Transactions on Wireless Communications*, vol. 3, no. 5, pp. 1543–1553, 2004.
[46] P. Marsch, W. Rave, and G. Fettweis, "Quasi-orthogonal stbc using stretched constellations for low detection complexity," in *2007 IEEE Wireless Communications and Networking Conference. IEEE*, pp. 757–761, 2007.
[47] V. Stocker R. Cornelius, A. Narbudowicz, M. J. Ammann, and D. Heberling, "Calculating the envelope correlation coefficient directly from spherical modes spectrum," in 2 *2017 11th European Conference on Antennas and Propagation (EUCAP)*, pp. 3003–3006, 2017.
[48] V. Stocker S. Blanch, J. Romeu, and I. Corbella, "Exact representation of antenna system diversity performance from input parameter description," *Electronics letters*, vol. 39, no. 9, pp. 705–707, 2003.
[49] V. Stocker A. Goldsmith, Wireless communications, 2005.
[50] V. Stocker E. Biglieri, R. Calderbank, A. Constantinides, A. Goldsmith, A. Paulraj, and H. V. Poor, MIMO wireless communications, 2007.

BIOGRAPHIES OF AUTHORS

M. Muhsin is a lecturer at Department of Telecommunication Engineering, Institut Teknologi Telkom Surabaya. He obtained Master and Bachelor Degree in Telecommunication Engineering from Telkom University (Indonesia) in 2017 and 2016, respectively. His researches are in fields of wireless communications, antennas, and signal processing. He is affiliated with IEEE member in Communications Society since 2016. Further info on his homepage: https://muhsin.lecturer.ittelkom-sby.ac.id/

Afina Lina Nurlaili is a lecturer at Department of Informatics, Universitas Pembangunan Nasional "Veteran" Jawa Timur. She obtained Master and Bachelor Degree in Informatics from Institut Teknologi Sepuluh Nopember Surabaya in 2018 and 2016, respectively. Her researches are in fields of business process management, process mining, optimization, and general informatics.

Aulia Saharani is an undergraduate research assistant in Institut Teknologi Telkom Surabaya. Her assisted research are in wireless communications and antennas.

Indah Rahmawati Utami is an undergraduate research assistant in Institut Teknologi Telkom Surabaya. Her assisted research are in wireless communications and antennas.